Computers and Concrete, *Vol. 12, No. 2 (2013) 211-228*
DOI: http://dx.doi.org/10.12989/cac.2013.12.2.211

Elasto-plastic time history analysis of an asymmetrical twin-tower rigid-connected structure

Xiaohan Wu[1], Yanfei Sun*[1], Mingzhuo Rui[2], Min Yan[2], Lishu Li[2] and Dongze Liu[1]

[1]*College of Civil Engineering, Tongji University, Shanghai 200092, China*
[2]*East China Architectural Design & Research Institute Co., Ltd., Shanghai 200002, China*

(Received August 18, 2012, Revised February 20, 2012, Accepted March 5, 2013)

Abstract. The structure analyzed in this paper has particular building style and special structural system. It is a rigid-connected twin-tower skyscraper with asymmetrical distribution of stiffness and masses in two towers. Because of the different stiffness between the north and the south towers, the torsion seismic vibration is significant. In this paper, in order to study the seismic response of the structure under both frequent low-intensity earthquakes as well as rare earthquakes at the levels of intensity 7, the analysis model is built and analyzed with NosaCAD. NosaCAD is an nonlinear structure analysis software based on second-development of AutoCAD with ObjectARX. It has convenient modeling function, high computational efficiency and diversity post-processing functions. The deformations, forces and damages of the structure are investigated based on the analysis. According to the analysis, there is no damage on the structure under frequent earthquakes, and the structure has sufficient capacity and ductility to resist rare earthquakes. Therefore the structure can reach the goal of no damage under frequent earthquakes and no collapse under rare earthquakes. The deformation of the structure is below the limit in Chinese code. The time sequence and distribution of damages on tubes are reasonable, which can dissipate some dynamic energy. At last, according to forces, load-carrying capacity and damage of elements, there are some suggestions on increasing the reinforcement in the core tube at base and in stiffened stories.

Keywords: multi-tower structure; elasto-plastic time history analysis; seismic performance; complex building

1. Introduction

In the recent years, a large amount of tall buildings have been constructed in Mainland China. In order to make the design unique and add beauty to cities, many new buildings have novel architectural styles, such as the China Pavilion for Expo2010 Shanghai (Yang *et al*. 2010), multi-tower connected structure (Lu *et al*. 2009). However, irregularity and complexity of structures are inevitable for these special buildings. From past experiences, structural irregularities could cause severe damage or collapse under strong earthquakes. Therefore, it requires structural engineers to

*Corresponding author, Postgraduate Student, E-mail: sunyanfei1988@163.com

http://www.techno-press.org/?journal=cac&subpage=8 ISSN: 1598-8198(Print), 1598-818X (Online)

understand how these structures respond, especially in future earthquakes.

The seismic response of complex and irregular buildings has been theoretically investigated by several researchers (La De Llera and Chopra 1995, Das and Nau 2003, Tremblay and Poncet 2005). Most of these studies focus on seismic performances of multi-story reinforced concrete (RC) or steel buildings. For the experimental studies on irregular high-rise buildings, Lu *et al*. (1999) studied the dynamic response of a complex structure with U-shaped floors and specially shaped slant columns. Ko and Lee (2006) preformed a shaking table test on a 1/12-scale model to investigate the seismic performance of a 17-story high-rise RC structure with a high degree of torsional eccentricity and soft-story irregularity in the bottom of two stories. Lu *et al*. (2009) carried out shaking table model tests on a complex high-rise building with two towers of different heights connected by trusses. Besides theoretical and experimental investigation, with the development of software and personal computer, nonlinear analysis for complex irregular buildings has gradually come to maturity. Krawinkler (2006) believes that earthquake engineering is relying more and more on nonlinear analysis as a tool for evaluating structural performance and nonlinear analysis will be a good trend. Yahyai *et al*. (2009) used finite element model analysis to study the nonlinear seismic response of Milad Tower. Epackachi *et al*. (2010) conducted a seismic evaluation of a 56-story residential reinforced concrete building based on nonlinear dynamic time history analysis.

NosaCAD is an nonlinear structure software based on second-development of AutoCAD with ObjectARX. The process of model establishment and calculation are carried out in AutoCAD environment. It has convenient modeling function, high computational efficiency and diversity post-processing function. Many researchers used NosaCAD to consider the seismic performance of buildings. Wu *et al*. (2008) used the elastio-plastic time history analysis by NosaCAD to consider the seismic performance of the T2 building of Shanghai Pudong International Airport. Sun *et al*. (2009) made a research on earthquake resistance behavior of a long-span and cantilevered structure subjected to vertical motion by NosaCAD. Zhang *et al*. (2012) considered the seismic performance of a structure with irregularity in plan by NosaCAD. And Wu and Wei (2011) did an elasto-plastic time history analysis of a double-tower connected structure, analysis results from NosaCAD were compared with the results from shaking table test, the natural vibration frequencies of the structure were similar, the maximum drifts of the structure under earthquakes in experiment and analysis of NosaCAD were similar, too. They validated that the model built in NosaCAD was correct and the analysis results were believable.

In this paper, elasto-plastic time history analysis is conducted on a connected twin-tower skyscraper building called Gate of the Orient, which is specially designed with a gate-style shape. The height of this building exceeds the specified maximum height of 190 m for SRC frame and RC core wall system in Chinese code, and the fundamental vibration mode has a torsional component. So it belongs to code-exceeding design.

Three main parts are included in this paper. First, a refined finite element analysis model of this building is developed by NosaCAD. Then, nonlinear dynamic time history analysis about the complex building under frequent and rare earthquakes is adopted. Finally, the nonlinear dynamic responses such as displacement, inter story drift and damage of main lateral brace are presented and discussed. Moreover, practical suggestions are proposed on the basis of analysis.

2. Description of the structure

The gate-style joining twin tower skyscraper, the Gate of the Orient, with its grand arch, is located in the eastern end of the central business district in Suzhou Industrial Technology Park, at

Fig. 1 Perspective view of the structure

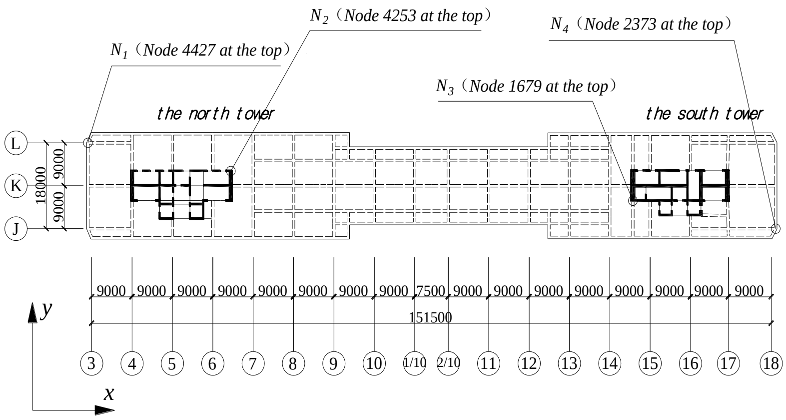

Fig. 2 59th north tower and 65th south tower plan

the west coast of Golden Cock Lake, Su Zhou, China. The building houses a 5 star hotel and a platinum 5 star hotel, office accommodation and a serviced apartment, the total construction area is 453142 m^2, including the underground parts. The main building is composed of two high-rise towers (Figs. 1-3). The total height is 278.0 m, and height of the connection is 228.9 m. Because of the different functional requirements, they differ in their stories, layout and service loads, hence their structural arrangement and weights differ, too.

The steel reinforced concrete frame and the reinforced concrete core wall system can resist lateral and vertical loads. Belt trusses are arranged at the height of 53.3 m, 114.9 m, 176.5 m and 288.9 m respectively, combined with the stiffened stories. It is the stiffness of the belt trusses that most strongly affects the overall behavior of the structure. In order to connect the core tube and

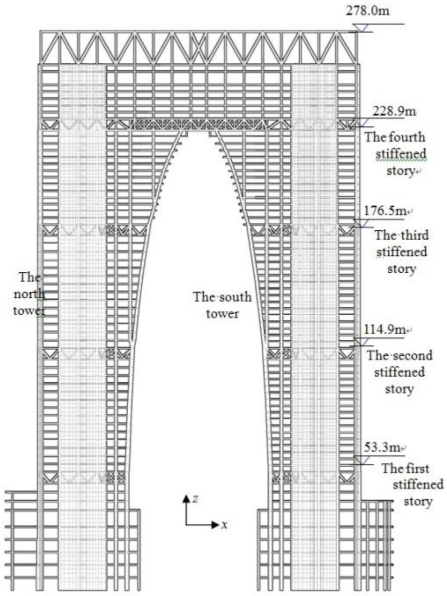

Fig. 3 Structure elevation

Table 1 Sections of the structural components

Location of components	Width and height of frame columns b×h/mm		Tickness of core tube d/mm	
	Tower center	Tower periphery	The north tower	The south tower
Below the first stiffened story	1400×2800	1200×1200	800	850
Between the first and the second stiffened story	1400×2500	1200×1900	800	850
Between the second and the third stiffened story	1000×1400	1000×1200	750	800
Between the third and the fourth stiffened story	1000×1000	600×1000	750	750
Above the fourth stiffened story	600×800	600×800	750	500

belt trusses in the stiffened stories, outrigger trusses are set at the corners of the core tube. I-section welded steels or profiled steel beams with 500~550 mm height and 200~400 mm width in section are applied as floor beams. And truss chords of the stiffened stories are welded square pipes with800 mm×500 mm in section and 30 mm in thickness.

Below the second stiffened story, rectangular steel reinforced concrete columns are used, the steel ratio of those is from 6% to 10%; and above the second stiffened story, rectangular steel pipe columns are employed in the exterior frame. Embedded steel reinforced concrete columns are set in the corners of the tube.

In order to form the arch gate shape, multiple oblique columns are arranged. The oblique columns are set up straight to the fourth stiffened story and the connecting parts, so that the vertical load of the connecting parts can be transferred to the base effectively, so the complex

Table 2 Material design strength of structural components

Location of components	Material	Compressive strength /MPa	Tensile strength /MPa
Columns and core tube below 94.8 m	C60	27.5	2.04
Columns and core tube between 94.8~156.4 m	C55	25.3	1.96
Columns and core tube between 156.4~182 m	C50	23.1	1.89
Columns and core tube between 182~234.m	C40	19.1	1.71
Columns and core tube above 234m and all floor slabs	C30	14.3	1.43
Steel beams, steel trusses、shape steels	Q345B	345*	345*

Note: *means steel yield strength

load transfer can be prevented in connecting parts.

To coordinate the displacement of the two towers at top, space trusses are arranged at the fourth stiffened story to form rigid connecting structure system.

Section sizes of the structural components are listed in Table 1. The material design strength of structural components is listed in Table 2.

According to the Chinese Code for Seismic Design of Building (CCSDB, GB50011-2001) (Ministry of Construction of the People's Republic of China 2001) and Technical Specification for Concrete Structures of Tall Building (TSCSTB, JGJ3-2002) (Ministry of Construction of the People's Republic of China 2002), the main characteristics of this structure, which are beyond the limitation of Chinese code, can be summarized as follows

(1) The height of this building exceeds the specified maximum height of 190 m for SRC frame and RC core wall system.

(2) According to TSCSTB, the ratio of torsional period and the first translational period is required to be less than 0.9 to prevent excessive torsional response. However, because of the different stiffness between the two towers, the fundamental vibration mode has a torsional component and there are rich torsion components in the following modes.

(3) In the elevation, the Gate of the Orient is a two-tower-connected hybrid structure. There are no experiences to build such a structure with two different stiffness towers connected.

3. Finite element model

NosaCAD (version 2010) was used to build the finite element model and carried out nonlinear dynamic time history analysis

3.1 Finite element model for structural components

Frame element model is consisted of three different stiffness regions, one is a linear elastic egion in the middle of the element, and other two are elasto-plastic regions at both ends of the element (Fig. 4).

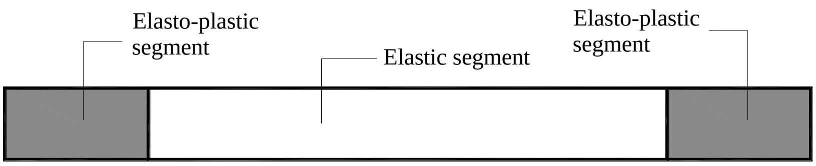

Fig. 4 The bar element with three stiffness regions

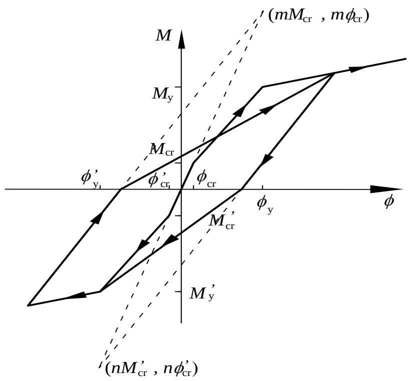

Fig. 5 Trilinear moment-curvature hysteretic model

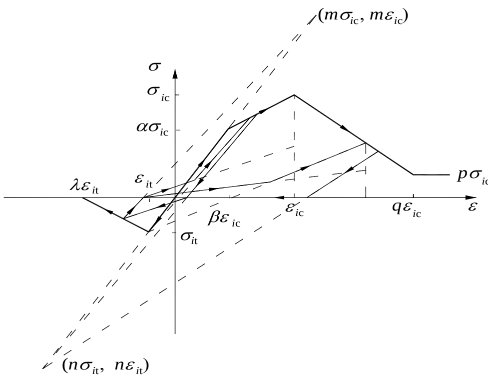

Fig. 6 Concrete constitutive model

For the frame members mainly suffer from bending moment, bilinear and trilinear moment-curvature hysteretic model are adopted for the elasto-plastic regions of steel beams, concrete beams and steel reinforced concrete beams, respectively. The frame element model only accounted for flexural effect in this paper. The trilinear moment-curvature hysteretic curve is shown in Fig. 5, in this model, *m* and *n* are 5.0.

For the nonlinear diaphragm, an orthogonal anisotropic concrete model based on equivalent uniaxial stress and strain relationship is adopted (Darwin and Pecknold 1976) together with a biaxial strength envelope (Kupfer and Gerstle 1973). The material model used for concrete is Darwin-Pecknold model. Concrete constitutive model is as shown in Fig. 6.

Fiber model is introduced to describe the nonlinear behavior in the elasto-plastic regions of the column. The ideal elastic-plastic constitutive model, accounting for yield hardening, is adopted for steel and rebar. Fiber model is also adopted to simulate the elasto-plastic behavior of trusses. The fiber model used in this paper is displacement-based fiber model. First, the sections of members are divided into small regions (namely fibers), then basing on plane cross-section assumption strain of every fiber is calculated according to the axial deformation, bending deformation and the position in section. And then the stress and elastic modulus of fiber are obtained by material uniaxial stress- strain hysteresis relationship, at last the force (3.1-1) and stiffness (3.1-2) of the whole cross section can be obtained by integral. N is the axial force, and M_x and M_y are bending moments, n is the total number of the fibers. i_c is the number of concrete fiber, (x_{ic}, y_{ic}) is its position, A_{ic} is its area, $(E_t)_{ic}$ is the tangent modulus of concrete fiber, and ε, (ϕ_x), $(\phi_y)_t$ are the characteristics of the section's deformation. The corresponding symbols of subscript "s" belong to rebar fibers.

$$N = \sum_{i_c=1}^{n_c} \left\{ (E_t)_{i_c} \left[\varepsilon_t + (\phi_x)_t y_{i_c} - (\phi_y)_t x_{i_c} \right] A_{i_c} \right\} + \sum_{i_c=1}^{n_c} \left\{ (E_t)_{i_s} \left[\varepsilon_t + (\phi_x)_t y_{i_s} - (\phi_y)_t x_{i_s} \right] A_{i_s} \right\} \tag{3.1-1a}$$

$$M_x = \sum_{i_c=1}^{n_c} \left\{ (E_t)_{i_c} \left[\varepsilon_t + (\phi_x)_t y_{i_c} - (\phi_y)_t x_{i_c} \right] A_{i_c} y_{i_c} \right\} + \sum_{i_s=1}^{n_c} \left\{ (E_t)_{i_s} \left[\varepsilon_t + (\phi_x)_t y_{i_s} - (\phi_y)_t x_{i_s} \right] A_{i_s} y_{i_s} \right\} \tag{3.1-1b}$$

$$M_y = \sum_{i_c=1}^{n_c} \left\{ (E_t)_{i_c} \left[\varepsilon_t + (\phi_x)_t y_{i_c} - (\phi_y)_t x_{i_c} \right] A_{i_c} \left(-x_{i_c} \right) \right\} + \sum_{i_s=1}^{n_c} \left\{ (E_t)_{i_s} \left[\varepsilon_t + (\phi_x)_t y_{i_s} - (\phi_y)_t x_{i_s} \right] A_{i_s} \left(-x_{i_s} \right) \right\} \tag{3.1-1c}$$

$$\left[K^{\mathrm{sect}} \right] = \begin{bmatrix} \sum_{i=1}^{n} (E_t)_i A_i & \sum_{i=1}^{n} (E_t)_i A_i y_i & -\sum_{i=1}^{n} (E_t)_i A_i x_i \\ \sum_{i=1}^{n} (E_t)_i A_i y_i & \sum_{i=1}^{n} (E_t)_i A_i y_i^2 & -\sum_{i=1}^{n} (E_t)_i A_i x_i y_i \\ -\sum_{i=1}^{n} (E_t)_i A_i x_i & -\sum_{i=1}^{n} (E_t)_i A_i x_i y_i & \sum_{i=1}^{n} (E_t)_i A_i x_i^2 \end{bmatrix} \tag{3.1-2}$$

Concrete constitutive model in fiber model is as shown in Fig. 6, ($m\sigma_{ic}$, $m\varepsilon_{ic}$) and ($n\sigma_{it}$, $n\varepsilon_{it}$) are the track curvature localization of the tensile region and compression region respectively. α is 0.7 and β is 0.4, p is 0.2, q is 3.0, m and n are 4.0, λ is 0.7.

For high-rises buildings, although there is torsional response on complete structures, but in per unit length of columns the torsion is small. The finite element model doesn't account for the

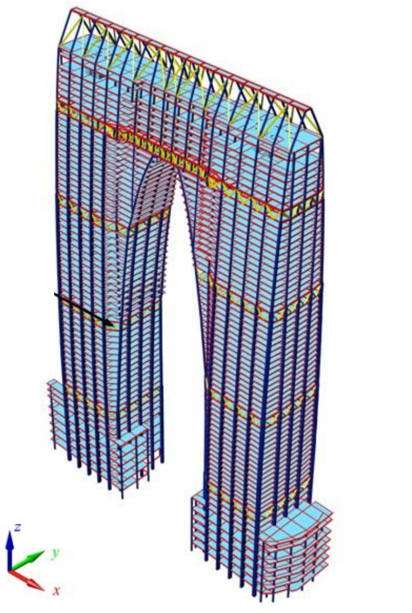

(a) Integral model

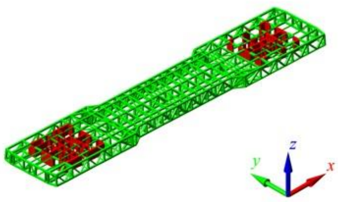

(b) The fourth stiffened story

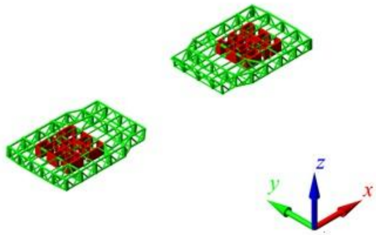

(c) The third stiffened story

Fig. 7 Analytical model of structure

torsion effect in columns and walls. Besides, there is no frame element model accounting for bending-torsional coupling effectively at present.

The relevant parameters of elastic-plastic analysis of the elements, such as cross-section parameters of fiber model and bending moment-curvature curve parameters are generated by

NosaCAD according to sectional geometric parameters, material parameters and reinforcement, etc.

The flat shell finite element, which is composed of diaphragm and plate, is used for shear wall and slab. The flat shell finite element model possesses rotational degrees of freedom in diaphragm, so that coupling beam element can be connected to shear wall with compatibility of deformation. In the nonlinear shell element, only the nonlinear property of the diaphragm is taken into account and the plate is regarded as linear. Meanwhile, rebar is supposed to dispersed in the element, it means that, to consider the effect of rebar, increase the concrete element in strength and stiffness according to the reinforcement ratio, actually there is no rebar element in the sections. The concrete hysteresis curve of equivalent uniaxial stress-strain relationship is the same as that in fiber model, and furthermore, the influence of the stress in orthogonal direction is considered. The ideal elastic-plastic model, taking into account the yield hardening, is still adopted for the reinforcement. It is assumed the smeared cracking is initiated once the tensile strength is reached and the second crack is permitted to appear orthogonal to the first one. This flat shell finite has been used for shear wall analysis under cyclic loading (Wu and Lu 1996) and prestressed concrete beam analysis (Wu and Lu 2003), effectively.

3.2 Analytical model of the structure

On the benefit of the graphical editing function of AutoCAD, the complex analytical model of the structure was built efficiently. It was composed of nonlinear elements of beams, columns, trusses and shear walls. Flat shell element was adopted for shear walls. Floor slabs based on the assumption of elastic floor was modeled by elastic flat shell elements. The structural model is shown as Fig. 7.

4. Nonlinear time history analysis

4.1 Input ground motions

According to the CSDB, the soil in Suzhou belongs to type III, which is defined that the overlaying thickness of the site is more than 50 m, and the average velocity of shear wave in the soil layer is between 140 and 250 m/s. It is specified in TSCSTB that at least two earthquake records and a synthetic accelerogram should be selected for elasto-plastic time history analysis. Considering the power spectral density properties of type III site soil, three different ground motions were applied as input accelerations to the model: (a) the El Centro record from the California Imperial Valley earthquake on 18 May 1940; (b) the Pasadena record from the California Kern County earthquake on 21 July 1952; and (c) the Nanjing synthetic record (NJW1 as shown in Fig. 8), which is formed according to the CSDB.

According to CSDB, buildings in seismic regions should be designed to sustain earthquakes of frequent, moderate and rare levels, which correspond to 63.2%, 10% and 2% probability of being exceeded in 50 years, and return period of 50, 475 and 2475 years, respectively. Suzhou belongs to the seismic zone of intensity 6.5 (roughly equivalent to a modified Mercalli intensity of 6.5). In order to investigate the structure seismic potential and study structure seismic performance in detail, higher intensity, intensity 7 (roughly equivalent to a modified Mercalli intensity of 7) was considered in this paper, the peak ground accelerations (PGAs) corresponding to the earthquakes

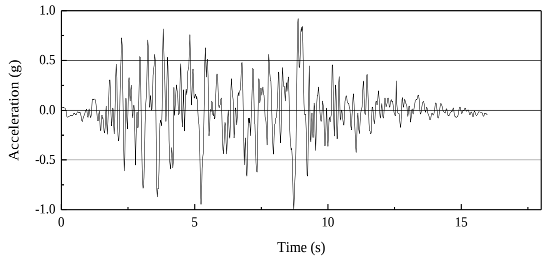

(a)

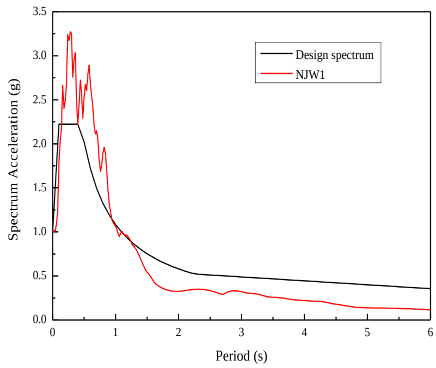

(b)

Fig. 8 NJW1 accelerogram: (a) time history of acceleration, and (b) response spectrum comparing to the design spectrum in CSDB Code

of frequent, moderate and rare levels are specified to be 0.035, 0.100 and 0.220 g, respectively.

Since seismic performance under rare earthquake was mainly investigated in this paper and no damage on the structure under frequently earthquake must be guaranteed, the peak ground acceleration (PGA) of selected earthquake accelerograms were scaled to 0.035 g and 0.220 g, corresponding to earthquakes of frequent and rare levels. During the analysis, the El Centro record and Pasadena record were inputted in two directions (X and Y direction in Fig. 7) simultaneously. The stiffness of the structure in Y direction is smaller than X, so Y direction is the principal direction, the ratio of PGA in Y direction to PGA in X direction is 1:0.85. And the Nanjing artificial record was inputted in one direction (X and Y direction separately).

As specified by TSCSTB, a damping ratio of 0.04 for SRC frame–RC core wall structural system was adopted, and Rayleigh damping was used in integration equation.

5. Analytical results

5.1 Input ground motions

Fig. 9 shows first three mode shapes were calculated by NosaCAD. Many kinds of structural analysis softwares were used to calculate, analyze and compare the free vibration properties and the elastic responses under earthquakes shown in Table 3. Because of the difference of the two

Table 3 Natural vibration period of structure

Order	Period (s)				Description
	NosaCAD	SATWE	ETABS	ANSYS	
1	6.170	5.974	5.722	5.980	Translation in direction Y with torsion
2	5.288	5.308	5.054	5.475	Torsion
3	4.831	5.036	4.730	5.245	Translation in direction X
4	2.275	2.271	2.094	2.459	Torsion in single tower
5	2.194	2.176	1.997	2.278	Torsion in single tower
6	1.783	1.931	1.809	2.248	The second translation in direction X

Table 4 The maximum displacement responses of node 4427

Seismic wave		Displacement in *x* direction /mm	Displacement in *y* direction /mm
Frequent intensity	El Centro	26.4	104.7
	Pasadena	14.1	23.1
	NJW1 in *x* direction	55.8	-
	NJW1 in *y* direction	-	68.0
Rare intensity	El Centro	108.7	549.7
	Pasadena	40.2	90.8
	NJW1 in *x* direction	292.6	-
	NJW1 in *y* direction	-	381.3

Table 5 Maximum extent of inter story drift at position *N*1 and *N*4

Seismic wave		Maximum extent of inter story drift	
		Position *N1*	Position *N4*
Frequent intensity	El Centro	1/1740	1/1705
	Pasadena	1/2448	1/2965
	NJW1 in *x* direction	1/1947	1/2091
	NJW1 in *y* direction	1/2310	1/2283
Rare intensity	El Centro	1/268	1/299
	Pasadena	1/1144	1/1032
	NJW1 in *x* direction	1/633	1/638
	NJW1 in *y* direction	1/402	1/457

towers, the fundamental vibration mode contains torsional component. It can also be found from the first mode shape that the stiffness of the north tower is less than another. One of the reasons is that the height of the typical floor of the north tower is larger and strength in connection between the core and frame in the south tower is greater. Because of the height, long period, significant influence of high order vibration modes, pushover analysis cannot be used effectively, instead, elasto-plastic time-history analysis is used to analyze response of the structure under earthquake.

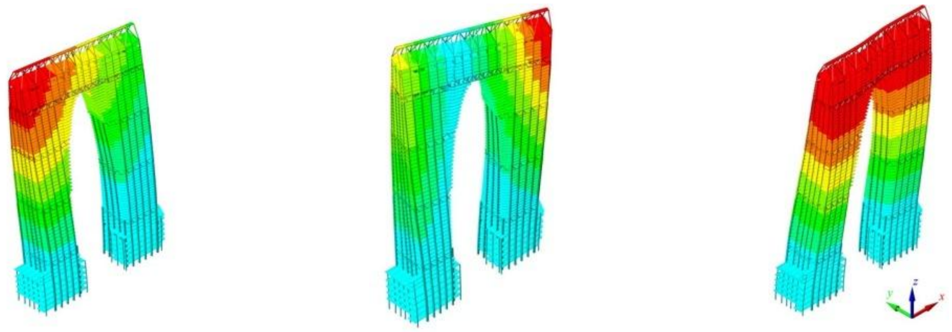

(a) The first vibration mode (c) The second vibration mode (e) The third vibration mode

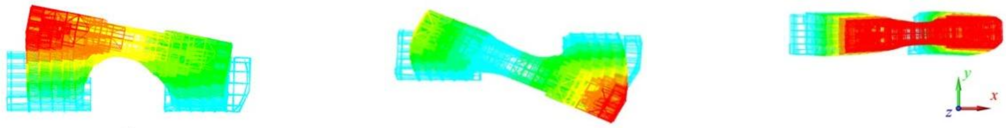

(b) Plane projection of the first vibration mode (d) Plane projection of the second vibration mode (f) Plane projection draw of the third vibration mode

Fig. 9 First three vibration modes of the structure

5.2 Roof displacement

The displacement response of the structure in y direction is larger than that in x direction. In addition to the first vibration mode, the participation of high order vibration modes is obvious in the displacement responses, which are accompanied by some torsion.

Figs. 10 and 11 show the displacement response history of node 4427, which located in the roof corner (Fig. 2). The maximum extents of displacement time history at node 4427 are listed in Table 4.

Fig. 12 shows the comparison of the displacement response history of node 4427 and node 2373, which located in the corner of south tower roof (Fig. 2), in Y direction under rare intensity 7 of El Centro. Because of the larger stiffness, the displacement response on the south tower roof lagged behind that on the north tower roof.

5.3 Inter storey drift

For the elastic diaphragm hypothesis was applied in these floor model, the strings of nodes along the vertical direction at positions N1, N2, N3 and N4 (Fig. 2) were chosen to investigate the inter story drift. N1 and N2 were on the north tower, while N3 and N4 were on the south tower. The maximum deformations generated by El Centro under frequent intensity and rare intensity, are shown in Fig. 13. It can be found that the inter story drift regresses near the height of 53.3 m, 114.9 m, 176.5 m and 228.9, where four stiffened stories were set. The stiffened stories reduce the lateral deformation effectively and avoid the accumulation of the deformation from bottom to top.

Maximum inter story drift at position N1 and N4 are listed in Table 4.

Fig. 14 shows the comparisons of the story drift envelops of elastic and elasto-plastic analysis. Under frequent earthquake, the story drift envelops are barely noticeable difference between the elastic and elasto-plastic results, which means there is almost no damage on the structure. Under

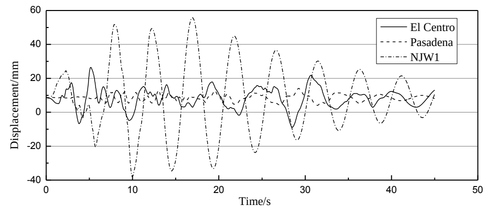

(a) *x* direction

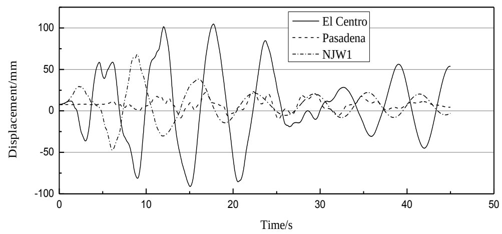

(b) *y* direction

Fig. 10 Displacement time history of the node 4427 under frequent intensity 7

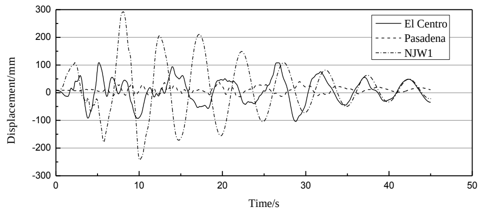

(a) *x* direction

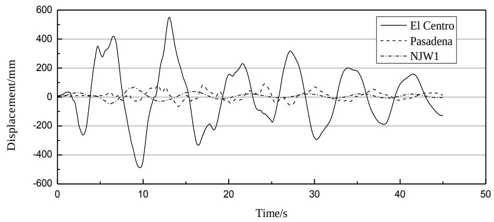

(b) *y* direction

Fig. 11 Displacement time history of the node 4427 under rare intensity 7

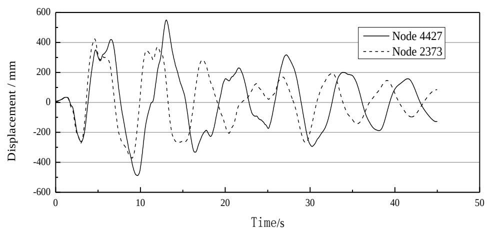

Fig. 12 Displacement time history of the node 4427 and 2373 in *y* direction under rare intensity 7 El Centro

rare earthquake, the story drift envelops of the north tower under elastic analysis are almost as same as that under elasto-plastic analysis, while the difference of story drift envelops at the lower part of the south tower are obvious, which means there is more plastic behavior in the lower part of the south tower, there are more cracks at the lower part of south tower shown as Fig. 14(b).

5.4 Damage patterns

Under the simulations of the frequent earthquakes of intensity 7, there is no damage in the structure. It can meet the code requirements of no damage under frequent earthquakes.

Considering the structural response of El Centro is more significant than that of the other two, responses generated by El Centro are taken into illustrate the damage development in the structure under rare earthquakes in detail.

The structure was elastic in the first 2 s. From 2.31 s on, plastic deformation began to occur in the coupling beams of 6th north tower story. Then the coupling beams were progressively damaged from 6th north tower story to its adjacent stories. When it came to 2.74 s, damage came out in the coupling beams of the 5th south tower story. About the same time, the coupling beams of north tower stories adjacent to the roof yielded. At 2.93 s coupling beams of south tower stories adjacent to 4th stiffened story yielded. From then on, the coupling beams of two towers came into yielding progressively and the concrete of some the coupling beams were crushed. There is no plastic deformation in other elements. The cracks mainly occurred in the core tube walls adjacent to the stiffened stories, the setback at the top of the fourth stiffened story and bottoms of the towers. There is no yielding of reinforcement and no crush of concrete in the tube walls. Fig. 15 shows the damage patterns of two tubes under the rare earthquake of El Centro.

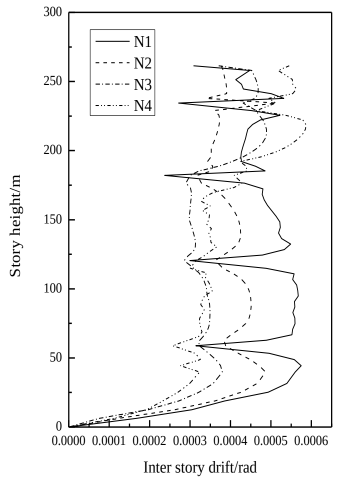

(a)

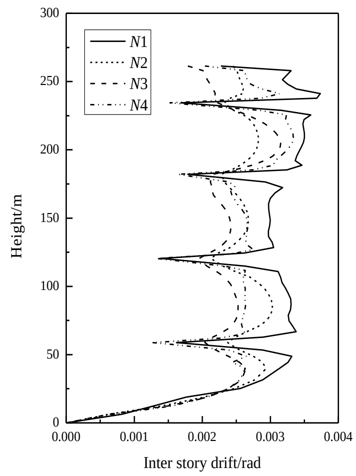

(b)

Fig. 13 (a) Inter story drift envelops under frequent intensity 7 El Centro (b) Inter story drift envelops under rare intensity 7 El Centro

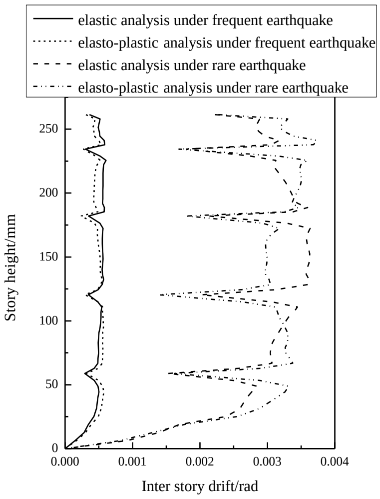

(a) The north tower

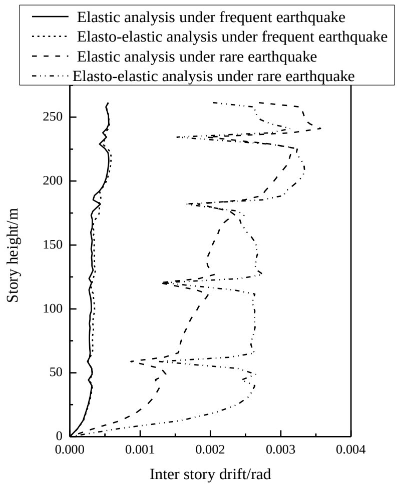

(b) The south tower

Fig. 14 Inter story drift envelops of elastic and elasto-plastic model under El Centro

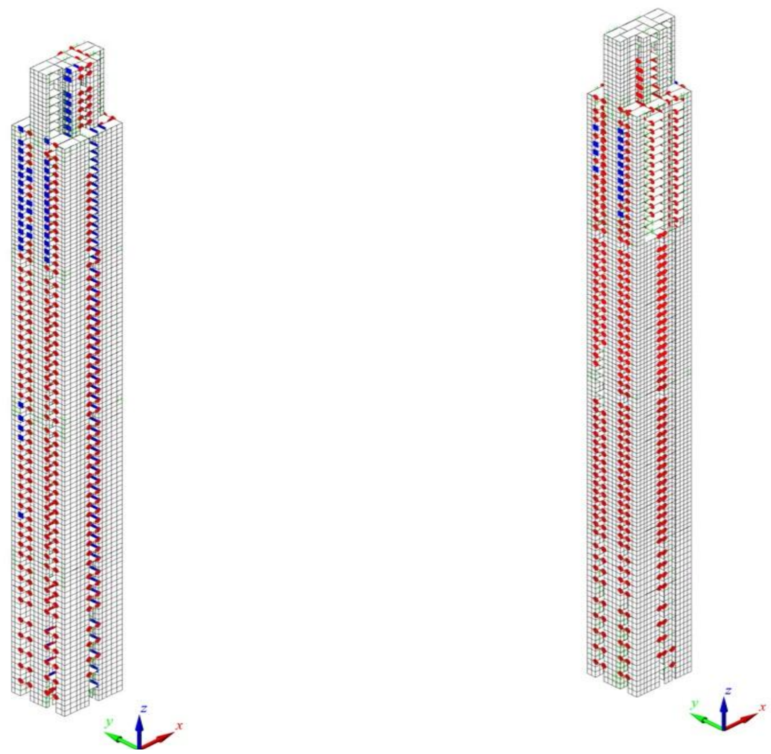

/——Concrete cracked. ●——Plastic hinge or rebar yielded. ■——Concrete crushed

Fig. 15 Damage patterns of tubes under rare intensity 7 El Centro

Table 6 Base shear and the ratio of base shear to weight (*x* direction)

Seismic wave		Base shear of the north tower/kN	Percentage /%	Base shear of the south tower /kN	Percentage /%	Base shear of all/kN	ratio of base shear to weight /%
Frequent intensity	El Centro	9.92×10^{3}	47.04	1.12×10^{4}	52.96	2.11×10^{4}	0.68
	Pasadena	8.42×10^{3}	47.51	9.32×10^{3}	52.49	1.77×10^{4}	0.57
	NJW1 in *x* direction	1.50×10^{4}	46.16	1.72×10^{4}	53.84	3.26×10^{4}	1.05
Rare intensity	El Centro	6.14×10^{4}	47.35	6.83×10^{4}	52.65	1.30×10^{5}	4.18
	Pasadena	5.14×10^{4}	47.56	5.67×10^{4}	52.44	1.08×10^{5}	5.91
	NJW1 in *x* direction	1.01×10^{5}	47.31	1.13×10^{5}	52.69	2.14×10^{5}	6.90

Annotation: the basal shear listed in Table 6 has removed the influence of the initial load

Table 7 Base shear and the ratio of base shear to weight (*y* direction)

Seismic wave		Base shear of the north tower/kN	Percentage /%	Base shear of the south tower /kN	Percentage /%	Base shear of all/kN	Ratio of base shear to weight /%
Frequent intensity	El Centro	1.88×10^{4}	53.13	1.66×10^{4}	46.87	3.54×10^{4}	1.14
	Pasadena	6.32×10^{3}	38.88	9.94×10^{3}	61.13	1.63×10^{4}	0.52
	NJW1 in *y* direction	1.22×10^{4}	40.94	1.76×10^{4}	59.06	2.98×10^{4}	0.96
Rare intensity	El Centro	7.33×10^{4}	40.05	1.10×10^{5}	59.95	1.83×10^{5}	5.91
	Pasadena	4.70×10^{4}	48.45	5.00×10^{4}	51.55	9.70×10^{4}	3.12
	NJW1 in *y* direction	6.94×10^{4}	41.76	8.68×10^{4}	58.24	1.56×10^{5}	5.02

Annotation: the basal shear listed in Table 7 has removed the influence of the initial load

5.5 Base shear

The base shear and the ratio of base shear to weight when subjected to different ground motions are listed in Table 6 and Table 7. It is clear that a difference exists between structural responses to the three inputs, in which responses under El Centro and NJW1 are greater than that under Pasadena. This is true not only for the maximum base shear but also for roof displacement results, which were discussed in the previous sections.

According to the CSDB, design seismic performance is determined by using seismic coefficient, which is derived from the acceleration response spectrum. In order to guarantee the safety of buildings, seismic shear factor is introduced. It is defined as the ratio of horizontal seismic shear force to the representative value of the gravity load of the structure, it is used to prevent the design seismic performance from being too small. Usually, there is a minimum value for seismic coefficient in seismic design code. As far as seismic protection intensity 7 is concerned, the factor should be no less than 0.016 for structures with obvious torsion effect or fundamental period of less than 3.5 s and 0.012 for structures with fundamental period greater than 5.0 s. Seismic shear factors at the ground floor of this structure satisfied the requirement of 1.2%.

6. Conclusions

The asymmetrical twin-tower rigid-connected structure is a steel-concrete hybrid high rise building. The building is extremely irregular in elevation. In this paper, elasto-plastic time history analysis was carried out to study the seismic performance of the building. Based on the detailed analysis of numerical study, conclusions are summarized as follows:

(1) The structure under frequent earthquakes mostly keeps elastic and the envelopes of the inter-story drift meet the code requirement.

(2) Under rare earthquakes, coupling beams could yield and dissipated seismic energy prior to the core walls, which realized a favorable energy dissipation mechanism and was helpful for reducing the damage on the lower part of the main structure.

(3) Under rare earthquakes, although plastic hinges occurred on the coupling beams, other vertical load-carrying members do not damage except that the tube wall cracks at the bottom and near the stiffened stories. Therefore the structure meets the current Chinese Code requirements of no damage under frequent earthquake and without collapse under rare earthquakes. The envelopes of the inter-story drift under a rare earthquakes also meet the code requirement of 1/100.

(4) For the reason of asynchronous between two towers, the torsional responses are obvious. However, connecting part of the structures above the forth stiffened story were strong enough and there was no damage under rare earthquakes.

(5) There was no damage on the oblique steel tube columns for supporting upper connecting parts and the columns were far from yield under rare earthquakes, the safety of connecting part can be guaranteed effectively.

(6) Stresses in the tube walls near stiffened stories is complex, especially in the setback of the fourth stiffened story, and the cracks mainly occurred at these positions under rare earthquakes. In order to reduce damage, increasing reinforcement of these parts is suggested.

References

Darwin, D. and Pecknold, D.A. (1976), "Analysis of RC shear panels under cyclic loading", *J. Struct. Div.* ASCE, **102**, 355-369.

Das, S. and Nau, M. (2003), "Seismic design aspects of vertically irregular reinforced concrete buildings", *Earthq. Spectra*, **19**, 455-477.

Epackachi, S., Mirghaderi, R. and Esmaili, O. (2010), "Seismic evaluation of a 56-story residential reinforced concrete high-rise building based on nonlinear dynamic time history analysis", *Struct. Des. Tall Spec*, **21**(4), 233-248.

Ko, D.W. and Lee, H.S. (2006), "Shaking table tests on a high-rise RC building model having torsional eccentricity in soft lower stories", *Earthq. Eng. Struct. Dyn.*, **35**, 1425-1451.

Krawinkler, H. (2006), "Importance of good nonlinear analysis", *Struct. Des. Tall Spec.*, ***15***, 515-531.

Kupfer, H.B. and Gerstle, K.H. (1973), "Behaviour of concrete under biaxial stresses", *J. Eng. Mech. Div. ASCE*, **99**, 853-866.

La De Llera, J.C. and Chopra, A.K. (1995), "Understanding the inelastic seismic behavior of asymmetric-plan buildings", *Earthq. Eng. Struct. Dyn.*, **24**(4), 549-572.
Lu, X.Z., Ye, L.P. and Liao, Z.W. (2009), *Elasto-plastic analysis of buildings against earthquake*, China Architecture &Building Press, 14-15.
Lu, X.L., Zhang, H.Y., Hu, Z.L. and Lu, W.S. (1999), "Shaking table testing of a U-shaped plan building model", *Can. J. Civ. Eng.*, **26**, 746-759.
Lu, X.L., Chen, L.Z., Zhou, Y. and Huang, Z.H. (2009), "Shaking table model tests on a complex high-rise building with two towers of different height connected by trusses", *Struct. Des. Tall Spec.*, **18**(7), 765-788.
Lu, X.L., Su, N.F. and Zhou, Y. (2011), "Nonlinear time history analysis of a super-tall building with setbacks in elevation", *Struct. Des. Tall Spec.*, **22**(7), 593-614.
Ministry of Construction of the People's Republic of China (2001), *Code for Seismic Design of Buildings (GB50011-2001)*, China Architecture and Building Press, Beijing, China.
Ministry of Construction of the People's Republic of China (2002), *Technical Specification for Concrete Structures of Tall Building (JGJ3-2002)*, China Architecture and Building Press, Beijing, China.
Sun, F.T., Wu, X.H. and Lu, X.L. (2009), "Research on earthquake resistance behavior of a long-span and cantilevered structure subjected to vertical motion", *Struct. Eng.*, **25**, 71-77.
Tremblay, R. and Poncet, L. (2005), "Seismic performance of concentrically braced steel frames in multistory buildings with mass irregularity", *J. Struct. Eng.*, **131**, 1363-1375.
Wu, X.H. and Lu, X.L. (1996), "Nonlinear finite element analysis of reinforced concrete slit shear wall under cyclic loading", *Journal of Tongji University*, **24**, 117-123.
Wu, X.H. and Lu, X.L. (2003), "Tendon model for nonlinear analysis of externally prestressed concrete structures", *J. Struct. Eng*., ASCE, **129**(1), 96-104.
Wu, X.H., Yuan, Z.Y. and Lu, X.L. (2008), "Elasto-plastic time history analysis of T2 building of shanghai pudong international airport", *J. Earthq. Eng*., **19**, 71-75.
Wu, X.H., Wei, X.D., Qian, J. and Lu, X.L. (2011), "Elasto-plastic time history analysis of a double-tower connected structure", *J. Earthq. Eng.*, **31**, 51-58.
Yahyai, M., Rezayibana, B. and Daryan, A.S. (2009), "Nonlinear seismic response of milad tower using finite element model", *Struct. Des. Tall Spec.*, **18**(8), 877-890.
Yang, J., Chen, Y., Jiang, H. and Lu, X. (2010), "Shaking table tests on china pavilion for expo 2010 Shanghai China", *Struct. Des. Tall Spec.*, **21**(4), 265-282.
Zhang, T., Wu, X.H. and Lu, X.L. (2012), "Elasto-plastic time history analysis of a structure with irregularity in plan", *Struct. Eng.*, **28**, 18-26.

CM